The Signature of a Correlation between $> 10^{19}$eV Cosmic Ray Sources and Large Scale Structure

Eli Waxman and Karl B. Fisher
Institute for Advanced Study, Princeton, NJ 08540

Tsvi Piran
Racah Institute for Physics, The Hebrew University, Jerusalem, 91904, Israel

ABSTRACT

We analyze the anisotropy signature expected if the high energy (above 10^{19}eV) cosmic ray (CR) sources are extra-Galactic and trace the distribution of luminous matter on large scales. We investigate the dependence of the anisotropy on both the relative bias between the CR sources and the galaxy distribution and on the (unknown) intrinsic CR source density. We find that the expected anisotropy associated with the large scale structure (LSS) should be detected once the number of CR events observed above 10^{19}eV is increased by a factor of ~ 10. This would require ~ 30 observation-years with existing experiments, but less then 1 year with the proposed ~ 5000 km^2 Auger detectors. We find that the recently reported concentration of the Haverah Park CR events towards the super-galactic plane is not consistent with the known LSS. If real, the Haverah Park result suggests that the CR sources are much more concentrated towards the super-galactic plane than the known LSS. Our results are not sensitive to the number density of CR sources. We show that once the number of detected events is increased by a factor of ~ 10, the number density would be strongly constrained by considering the probability for having repeating sources.

Subject headings: cosmic rays — large-scale structure of the universe

1. Introduction

Recent cosmic ray observations, reported by the Fly's Eye (Bird *et al.* 1994) and by the AGASA (Yoshida *et al.* 1995) experiments, show two major features in the cosmic ray (CR) energy spectrum above 10^{17}eV. First, a break in the shape of the spectrum is observed at $\sim 5 \times 10^{18}$eV. Second, the CR composition changes from being predominantly heavy nuclei below the break to light nuclei above the break. Coupled with the lack of anisotropy, that would be expected if the CRs above 10^{19}eV were protons produced in the Galaxy, these features strongly suggest that the CR flux above 10^{19}eV is dominated by an extra-Galactic component of protons. This view is supported by the fact that the CR spectrum above $\sim 2 \times 10^{19}$eV is consistent with

a cosmological distribution of sources, with a power law generation spectrum $\mathrm{d}\ln N/\mathrm{d}\ln E \simeq -2$ (Waxman 1995b,c) (below $\sim 2\times10^{19}$eV a significant contribution from iron cosmic rays from Galactic sources is likely to be present; Bird *et al.* 1994, Waxman 1995b).

If the particles observed are indeed protons of extra-Galactic origin, and if their sources are correlated with luminous matter, then the inhomogeneity of the large scale galaxy distribution, on scales $\lesssim 100h^{-1}$Mpc, should be imprinted on the CR arrival directions. In this paper, we examine the expected anisotropy signature if the CR sources trace the large scale structure (LSS), and investigate its dependence on the relative bias between the CR sources and the galaxy distribution and on the (unknown) intrinsic CR source density. The galaxy distribution is derived from the *IRAS* 1.2 Jy redshift survey (Fisher *et al.* 1995). We find that the expected anisotropy associated with the LSS should be detected once the number of CR events detected above 10^{19}eV is increased by a factor of ~ 10. Stanev *et al.* (1995) have recently noted that the arrival directions of $E > 4\times10^{19}$eV CR events detected by the Haverah Park experiment show a concentration in the direction of the Supergalactic Plane (SGP) which is inconsistent with the hypothesis that the CR sources are distributed isotropically. We confirm this result, but also find that the Haverah Park CR distribution is unlikely to be explained by the hypothesis that the CR sources trace the known LSS.

2. The angular distribution of CRs in a cosmological scenario

We consider a model where the CR flux is produced by a cosmological distribution of proton sources that trace the large scale galaxy distribution. We model the number density of CR sources in a comoving volume element $\mathrm{d}V$ at redshift z as drawn from a Poisson distribution with mean $\bar{s}(z)\,b[\delta\rho]\,\mathrm{d}V$, where $\bar{s}(z)$ is the average comoving number density of CR sources at redshift z and b is some (bias) functional of the local galaxy overdensity, $\delta\rho$. With this assumption, we are able to derive in §2.1 a closed analytic expression for the probability of observing a source which produces a specified number of events at a detector for a given exposure and sky coverage. In § 2.2, we apply this formalism to generate Monte-Carlo realizations of the CR distribution arising from a population of sources which trace the LSS seen in the *IRAS* redshift survey. In § 2.3, we analyze the anisotropy of CR arrival distribution and discuss the implications of our results for the observed anisotropy reported by Stanev *et al.* (1995). We conclude in § 3.

2.1. Formalism

As they propagate, high energy protons lose energy due to the cosmological redshift and due to the production of pions and e^+e^- pairs caused by interactions with microwave background photons. We denote by $E_0(E,z)$ the energy at which a proton must be produced at an epoch z in order to be observed at present ($z=0$) with energy E. With this definition, the CR flux

above energy E, produced by a source at redshift z, is given by $(1+z)\dot{N}[E_0(E,z)]/4\pi d_L(z)^2$, where $\dot{N}[E]$ is the rate at which the source produces protons above energy E and $d_L(z)$ is the luminosity distance. For simplicity, we assume that the sources are identical, so that $\dot{N}$ is given by the present ($z=0$) source number density, $\bar{s}_0$, and CR production rate per unit volume, $\dot{n}_0$, as $\dot{N}[E] = \dot{n}_0(E)/\bar{s}_0$ (Note, however, that it is straightforward to include a source luminosity function in our formalism). The number of detected CR events produced by a source at redshift z is modeled as a Poisson distribution with mean

$$\bar{N}(E,z) = \dot{N}[E_0(E,z)]\frac{(1+z)AT}{4\pi d_L(z)^2} = \frac{\dot{n}_0[E_0(E,z)]}{\bar{s}_0}\frac{(1+z)AT}{4\pi d_L(z)^2}, \tag{1}$$

where A and T are the detector area and observation time respectively.

If many faint sources produce the observed CR events, then a natural assumption would be that each source has a negligible probability of producing more than one event. However, the density of CR sources is as yet unknown and there is the possibility that the observed events are comprised in part of sources producing multiple events (repeaters). In the following derivation, we present a formalism which enables the probability that a source will produce one or multiple events to be calculated for a specified source density; the familiar notion of each source producing only one event is recovered in the limit of infinite source density.

The number of CR *sources* in a comoving volume element $\mathrm{d}V$ at redshift z is taken to be Poisson distributed with mean $\bar{S} = \bar{s}(z)b[\delta\rho]\mathrm{d}V$. The probability that a source would produce i detected CR events above energy E is $P_i(E,z) = \bar{N}(E,z)^i \exp[-\bar{N}(E,z)]/i!$. The probability that the number of sources producing 1 events is n_1, the number of those producing 2 events is n_2, and so on, is

$$\begin{aligned} P(\{n_i\}) &= \sum_{S=N}^{\infty} \frac{1}{S!}\bar{S}^S e^{-\bar{S}} \frac{S!}{(S-N)!\prod_i n_i!}\prod_i P_i^{n_i}\left(1-\sum_i P_i\right)^{S-N} \\ &= \left(\prod_i \frac{1}{n_i!}\right) e^{-\bar{S}} \prod_i (\bar{S}P_i)^{n_i} \sum_{S=N}^{\infty}\frac{1}{(S-N)!}\left[\bar{S}\left(1-\sum_i P_i\right)\right]^{S-N} \\ &= \prod_i \frac{1}{n_i!}(\bar{S}P_i)^{n_i} e^{-\bar{S}P_i} \quad , \end{aligned} \tag{2}$$

where $N = \sum_i n_i$. Thus, the number of sources producing i events is Poisson distributed with average $\bar{S}P_i$, and is statistically independent of the number of sources producing $j \neq i$ events. This implies that the number S_i of sources producing i events in a given angular region of the sky is Poisson distributed with average given by the sum of $\bar{S}P_i$ over all relevant volume elements, and that S_i is statistically independent of S_j for $i \neq j$. The average number per steradian of sources producing i events in the direction $\hat{\Omega}$ is given by

$$\bar{S}_i(E,\hat{\Omega}) = \int \mathrm{d}z\, c\left|\frac{\mathrm{d}t}{\mathrm{d}z}\right| \frac{d_L(z)^2}{1+z}\,\bar{s}(z)\, b[\delta\rho(z,\hat{\Omega})]\, P_i(E,z) \quad . \tag{3}$$

Equation 3 makes it easy to compute the mean number of sources producing a given number of events above a given energy and forms the basis for the Monte-Carlo method described in the next section. It is straight forward to show that the number per steradian of sources producing more than one detected CR above energy E, i.e. the number of repeaters, is Poisson distributed with average given by (3) with $P_i(E,z) = 1 - [1 + \bar{N}(E,z)]\exp[-\bar{N}(E,z)]$. The mean number per steradian of observed CR events is:

$$\bar{N}_o(E,\hat{\Omega}) = \frac{1}{4\pi} AT\dot{n}_0(E) \int \mathrm{d}z\, c \left|\frac{\mathrm{d}t}{\mathrm{d}z}\right| \frac{\bar{s}(z)}{\bar{s}_0}\, b[\delta\rho(z,\hat{\Omega})]\, \frac{\dot{n}_0[E_0(E,z)]}{\dot{n}_0(E)} \quad . \tag{4}$$

2.2. Monte-Carlo analysis of CR arrival directions

We now wish to exploit the formalism of the previous section by making specific Monte-Carlo realizations of CR arrival directions for a particular detector and exposure time. Equation 3 can be used to determine the mean number of sources along a particular line of sight which produce a given number of CR events, once the underlying cosmology, the source evolution $\bar{s}(z)$, the density field $\delta\rho$, and the biasing function, $b[\delta\rho]$, have been specified. For the numerical calculations of the rest of the paper we adopt the following cosmological scenario: flat universe with zero cosmological constant ($\Omega = 1,\ \Lambda = 0$), $H_0 = 100$km sec^{-1}Mpc^{-1}, and non-evolving sources ($\bar{s}(z) = \bar{s}_0$). Our results are not sensitive to the cosmological parameters ($\Omega,\ \Lambda$) and to source evolution, since CRs of energy $E > 4 \times 10^{19}$eV are produced by sources at distances smaller than 500 Mpc (see Fig. 1), which are short on a cosmological scale. The function $E_0(E,z)$ is numerically calculated under the above assumptions in a method similar to that described in Waxman 1995b. The proton spectrum generated by the sources is assumed to be a power law, $\dot{N}(E) \propto E^{-1}$, which is consistent with the observed CR spectrum above 2×10^{19}eV (Waxman 1995b).

Figure 1 presents the fraction of the differential CR flux, that is contributed by sources at distances $< d$, for a homogeneous distribution of CR sources, for several values of d (the results are obtained by numerically integrating equation (4) with $b \equiv 1$). The rapid energy loss due to pion production gives rise to the sharp cutoff with distance. CRs with energies $\gtrsim 8 \times 10^{19}$eV must originate from sources within $\lesssim 100$ Mpc. High energy CRs therefore offer a probe of the relatively local universe which is uncontaminated by distant sources. Searching for the signal of anisotropy associated with the LSS involves a compromise between diluting of the signal by working with lower energy events and increasing the statistical uncertainty by restricting the analysis to the rare high energy events.

We estimate the large scale galaxy density field by smoothing the galaxy distribution of the 1.2 Jy *IRAS* redshift survey (Fisher *et al.* 1995) with a variable Gaussian filter with a dispersion given by the larger of $6.4h^{-1}$Mpc and the mean galaxy separation (cf. Fisher *et al.* 1995). Variable smoothing is essential for maintaining high resolution nearby ($r \lesssim 25\ h^{-1}$Mpc) while simultaneously suppressing shot noise at large distances ($r \gtrsim 75\ h^{-1}$Mpc). The relatively large local smoothing length of 6.4 h^{-1}Mpc (corresponding to the same volume as a top-hat

filter of radius 10 h^{-1}Mpc) was chosen so that the smoothing length remains constant out to $\sim 100h^{-1}$Mpc. For distances $> 200\ h^{-1}$Mpc we have assumed a homogeneous ($\delta\rho = 0$) galaxy distribution. In the range $100 < r < 200\ h^{-1}$Mpc, the smoothing length increases from 15 h^{-1}Mpc to about 45 h^{-1}Mpc. At first glance, this degradation in resolution might appear worrisome. We tested the robustness of our results by augmenting our density field with realizations of the small scale structure consistent with the known *IRAS* power spectrum; the results reported in the following sections were found to be very insensitive to the lack of small scale resolution at large distances.

For the bias function, $b[\delta\rho]$, we consider three models: An isotropic (I) model, where the CR source distribution is purely isotropic, i.e. $b[\delta\rho] \equiv 1$; An unbiased (UB) model, where the CR sources trace the galaxy distribution with $b[\delta\rho] = 1 + \delta$; A biased (B) model where the CR source distribution is biased compared to the galaxy distribution with a simple threshold bias, $b[\delta\rho] = 1 + \delta$ for $\delta > \delta_{min}$ and zero otherwise. The value $\delta_{min} = 1$ produces a source distribution which is concentrated near the SGP in a manner very similar to that seen in nearby radio sources (Shaver & Pierre 1989). We therefore adopt $\delta_{min} = 1$ as our canonical "biased" model.

We generate a specific realization of CR arrival directions for a chosen model by dividing the sky into a set of angular bins; in each bin we draw the number of sources producing 1, 2, etc. events from Poisson distributions with means determined by equation (3). The product $AT\dot{n}_0(E)$ is fixed by requiring that the mean number of CRs produced match the number observed by a particular detector. Since we are interested only in large scale correlations of the CR sources with the galaxy distribution, we can use relatively coarse angular binning. We have adopted equal area bins of approximately $6^\circ \times 6^\circ$; this corresponds to the resolution of the *IRAS* density field at 100 h^{-1}Mpc and is comparable with the upper limits for deflections caused by inter-galactic magnetic fields. [The deflection angle for protons is (Waxman 1995a) $\theta_p \leq 5^\circ (d/100\ \mathrm{Mpc})^{1/2}/(E/10^{20}\mathrm{eV})$ for the current upper limit on inter-galactic magnetic field B with correlation length λ, $B\lambda^{1/2} \leq 10^{-9}$ G Mpc$^{1/2}$ (Kronberg 1994, Vallee 1990)]. The efficiency of CR detectors is usually a function of declination. Relative efficiencies can easily be accounted for by multiplying the mean counts in (3) by the appropriate weights. In the case of the Fly's eye detector, we model the efficiency as uniform above $\delta > -10^\circ$ with no sensitivity at smaller declinations.

Having specified the bias model, the only remaining parameter is the current source number density. We have performed our Monte-Carlo realizations using two values: $\bar{s}_0 = 10^{-2}\mathrm{Mpc}^{-3}$ and $\bar{s}_0 = 10^{-4}\mathrm{Mpc}^{-3}$. The high number density corresponds to the number density of bright galaxies. The low number density was chosen based on the following argument. The energy of the highest energy event detected by the Fly's Eye is in excess of 2×10^{20}eV (Bird *et al.* 1994). Since the distance traveled by such a particle can not exceed 50 Mpc (Aharonian & Cronin 1994), its detection implies that at least one CR source exists in the Fly's Eye field of view out to 50 Mpc, implying a source density $\bar{s}_0 > 10^{-5}$ Mpc^{-3}.

A more reliable lower limit to $\bar{s}_0$ may be given by considering the probability of observing repeating sources. As the source number density decreases, individual sources become brighter and, for a given number of detected events, the probability that one source would contribute more than one event increases. The analysis of §2.1 gives an analytic expression for the probability to observe a repeating source in a given angular bin. This is shown Fig. 2 which gives the probability that repeating sources would be observed (above an energy E) as a function of CR source density, $\bar{s}_0$, for the Fly's Eye exposure and the isotropic model. From Fig. 2, an absence of repeaters in the current Fly's Eye data above 5×10^{19}eV at the 90% confidence limit would imply a lower limit of $\bar{s}_0 > 10^{-5}\ \mathrm{Mpc}^{-3}$, similar to the lower limit inferred from the highest energy events. Clearly, the number density would be strongly constrained by considering repeating sources once the exposure is increased by a factor of ~ 10.

2.3. Results

Figures 3 and 4 present maps of the fluctuations in the mean CR intensity, $\Delta(E,\hat{\Omega}) \equiv 4\pi\bar{N}_o(E,\hat{\Omega})/\int d\hat{\Omega}\,\bar{N}_o(E,\hat{\Omega}) - 1$, for $E = 6,\ 4 \times 10^{19}$eV and the unbiased model. Also shown are the SGP and the Fly's Eye field of view for CRs with zenith angle $\theta < 45°$.[1] The map clearly reflects the inhomogeneity of the large-scale galaxy distribution- the over dense CR regions lie in the directions of the "Great Attractor" [composed of the Hydra-Centaurus ($l = 300$–$360°$, $b = 0$–$+45°$) and Pavo-Indus ($l = 320$–$360°$, $b = -45$–$0°$) superclusters] and the Perseus-Pisces supercluster ($l = 120$–$160°$, $b = -30$–$+30°$). The main structures of the CR arrival distribution, observable by northern hemisphere detectors such as AGASA and the Fly's Eye, are the overdensity in the Perseus-Pisces direction and the underdensity along the Galactic plane.

A crude estimate of the number of CR events required in order to detect these structures may be obtained as follows. For a given detector exposure the average number of events expected in the under-dense, $\Delta \lesssim -0.2$, region is 20% smaller in the UB model compared to the I model. If the number of expected events in both models is Poisson distributed, as would be the case for many faint sources ($\bar{s}_0 \to \infty$), then the probability that the I model would be ruled out at a 3σ level, assuming that the source distribution is described by the UB model, requires that the number of detected CRs, m, satisfy (for a $1-\sigma$ upward fluctuation) $0.8m + (0.8m)^{1/2} \lesssim m - 3m^{1/2}$, i.e. $m \gtrsim 300$. Since the $\Delta \lesssim -0.2$ region occupies $\sim 1/2$ the Fly's Eye field of view, this corresponds to a total of ~ 600 events. This number requires an exposure ~ 30 times higher than the current Fly's Eye exposure, for which ~ 20 events above 4×10^{19}eV were detected. A similar estimate is obtained considering the overdense region in the direction of the Perseus-Pisces supercluster.

In order to obtain a more accurate estimate of the exposure required to discriminated

[1]The choice of $\theta < 45°$ corresponds to the cut made by the CR experiments: The accuracy with which the CR energy and arrival direction is determined drops for larger zenith angle.

between the various models (I, UB, B) for the distribution of CR sources, we have considered the distribution of a statistic similar in spirit to χ^2,

$$X(E) = \sum_l \frac{[n_l(E) - n_{l,I}(E)]^2}{n_{l,I}(E)} \; . \tag{5}$$

Here n_l is the number of events detected in angular bin l and $n_{l,I}$ is the average number expected for the I model. For a total of ~ 100 observed CRs there would be, on average, 1 event per $15^\circ \times 15^\circ$ angular bin, limiting the angular resolution with which the overdensity map can be reconstructed to $\gtrsim 20^\circ$ (note, that the over/under densities predicted by the UB model are not large). Thus, for the calculation of X we have grouped the $6^\circ \times 6^\circ$ bins into $24^\circ \times 24^\circ$ bins. In addition, we have only used the 3 bins for which the UB model predicts the highest overdensity, and the 3 for which the model predicts the lowest underdensity. These bins cover $\sim 20\%$ of the Fly's Eye field of view, for which $|\Delta(E = 4 \times 10^{19}\text{eV}, \hat{\Omega})| \gtrsim 0.4$ in the UB model. It is clear from Fig. 4 and the arguments of the previous paragraph, that for the UB model the distribution of CRs in the remaining $\sim 80\%$ of the field of view, for which $|\Delta| \lesssim 0.2$, could not be discriminated from that expected in the I model for a total of only ~ 100 CR events.

The $X(E)$ distributions for the various models are shown in Fig. 5 for $E = 4,\ 6,\ 8 \times 10^{19}$eV and a detector with the Fly's Eye field of view and exposure for which 290 CRs above 4×10^{19}eV are detected, corresponding to ~ 10 times the current Fly's Eye exposure. The detector efficiency was assumed to be uniform within the field of view (corresponding to declination $> -10^\circ$). Clearly, there is a significant probability that this exposure would allow to discriminate between the models: The probability of ruling out the isotropic model at the $3-\sigma$ level, assuming that the CR sources are distributed as in the unbiased model, is $\gtrsim 15\%$; The probability for all other combinations (of assumed/ruled out model) is $\gtrsim 65\%$. It is unlikely that the $X(E)$ statistic could discriminate between the unbiased and isotropic models for an exposure significantly lower than 10 times the current exposure of the Fly's Eye detector. The biased model, however, could be discriminated from the isotropic model with only ~ 3 times the current Fly's Eye exposure.

Stanev *et al.* (1995) have recently noted a correlation between the arrival directions of $E > 4 \times 10^{19}$eV CR events detected by the Haverah Park experiment and the Supergalactic plane. Using our Monte-Carlo simulations we have calculated, following Stanev *et al.* (1995), the probability distribution of the absolute value and rms of the Supergalactic latitude, $|b^{SG}|$ and b^{SG}_{rms}, and Galactic latitude, $|b^G|$ and b^G_{rms}, for each of our bias models and for the two values of the source density, $\bar{s}_0$. The declination efficiency was derived from the declination distribution of the published Haverah Park events* with $E > 1 \times 10^{19}$eV and zenith angles less than 45°. The average number of events at each energy was chosen to correspond to that given in Stanev *et al.* (1995): 27 and 12 events above 4 and 6×10^{19}eV respectively. Table 1 presents the averages of $|b^{SG}|$, b^{SG}_{rms}, $|b^G|$, and b^G_{rms} obtained from the Monte-Carlo simulations of the various models, and the probability that a value smaller than the experimental Haverah Park value is obtained for each model.

In agreement with Stanev *et al.* (1995), we find that the probability to obtain the Haverah Park results assuming an isotropic CR source distribution is very low. [The slight differences between our numbers for the isotropic (I) model and those in Stanev *et al.* (1995) are due to the fact that we used a declination efficiency map and not the (unpublished) declinations of the observed events used in Stanev *et al.* (1995)]. However, we find that the probability to obtain the Haverah Park results is not significantly higher for models where the CR source distribution traces the LSS; thus, contrary to the claim by Stanev *et al.* (1995), we find that the concentration of the Haverah Park events towards the SGP is *not* strong support for the CR sources tracing the known LSS. It is important to note that for the biased model, where CR sources are restricted to high density regions in a way similar to radio galaxies, the probability to obtain the Haverah Park results is smaller than for the unbiased one. This reflects the fact that the superclusters, while concentrated towards the SGP, have offsets above and below the SGP which cause the inferred CR distribution to be less flattened than seen in the Haverah Park data.

As seen in Fig. 1, there is a significant contribution to the flux at 4×10^{19}eV from sources at distances $150 - 300$ Mpc, where the resolution of the galaxy density field inferred from the *IRAS* catalogue is fairly poor. The concentration of the Haverah park events toward the SGP might therefore be indicative of LSS at low Supergalactic latitude which is not seen in the *IRAS* galaxy distribution. In an effort to quantify this, we inserted an artificial supercluster at $r = 150h^{-1}$Mpc in the SGP with mass and size of the Shapley supercluster (Raychaudhury *et al.* 1991). This is most likely a worst case scenario since the actual Shapley cluster is seen (albeit outside the Haverah Park field of view) at a similar distance in the *IRAS* catalog and it is unlikely that any missed structure would lie precisely in the SGP. Even with such an extreme structure in the SGP, all of the models were unable to reproduce the concentration of the Haverah Park data at $\gtrsim 90\%$ confidence level. We conclude that the Haverah Park events either arise from sources concentrated in the SGP which are not probed by the known LSS or that there is some unknown systematic error in the positional accuracy of the CR events.

3. Discussion

We have shown that, if the distribution of CR sources trace the large scale structure, large exposure CR detectors should clearly reveal anisotropy in the arrival direction distribution of CRs above 4×10^{19}eV. The exposure required for a northern hemisphere detector to discriminate between isotropic CR source distribution and an unbiased distribution that traces the LSS is approximately 10 times the current Fly's Eye exposure. If the CR source distribution is strongly biased, the required exposure is ~ 3 times the current. Increasing the exposure by a factor of 10 with existing experiments (AGASA and Fly's Eye), would require ~ 30 years of observation (taking into account the fact that the AGASA experiment triggering was recently improved). The required observation time would be reduced if new, larger, CR experiments become operative: ~ 10 observation-years would be required with the new High Resolution Fly's Eye experiment

(Corbató *et al.* 1992), which is planned to become operative in two years; Less than 1 year of observation would be required if the proposed ~ 5000 km^2 detectors of the Auger project are built (Cronin 1992, Watson 1993).

An experiment with full sky coverage, such as the Auger experiment, would allow the CR event distribution to be analyzed conveniently in terms of a spherical multipole decomposition. In Fig. 6, we show the probability distribution for dipole and quadrupole moments of the CR distribution for a full sky coverage detector with an exposure ~ 100 times the current Fly's Eye exposure, comparable to the exposure of the Auger detectors after a few years of operation. The dipole moment has been defined as $D = \langle \cos\theta \rangle$ where θ is the angle between the CR position and fixed reference direction, taken to be $(l = 270^\circ,\ b = 30^\circ)$, while the quadrupole moment is defined as $Q = \langle \sin^2 b^G \rangle - \frac{1}{3}$. From the figure, it is evident that even these low order statistics are sufficient to discriminate between the models at a high degree of confidence. Moreover, since the various multipole moments are independent, the confidence level can be increased by including higher order moments of the CR distribution.

The anisotropy signal is not sensitive to the currently unknown number density of CR sources (see Figs. 5 and 6). We have shown, that a reliable lower limit to the source number density, $\bar{s}_0$, may be obtained by considering the probability of observing repeating sources. As the source number density decreases, individual sources become brighter and, for a given number of detected events, the probability that one source would contribute more than one event increases. An absence of repeaters in the current Fly's Eye data above 5×10^{19}eV, for example, would imply $\bar{s}_0 > 10^{-5}$ Mpc^{-3} with 90% confidence limit (see Fig. 2). The number density would be strongly constrained by considering repeating sources once the exposure is increased by a factor of ~ 10.

Stanev *et al.* (1995) have recently noted that the arrival directions of $E > 4 \times 10^{19}$eV CR events detected by the Haverah Park experiment show a concentration in the direction of the SGP. In agreement with Stanev *et al.* (1995), we find that the probability to obtain the Haverah Park results assuming an isotropic CR source distribution is very low. However, we find that this probability is not significantly higher for models where the CR source distribution traces the LSS; thus, contrary to the claim by Stanev *et al.* (1995), we find that the concentration of the Haverah Park events towards the SGP is *not* in strong support for the CR sources tracing the known LSS.

Our analysis addressed only the 2-dimensional (angular) LSS information contained in the distribution of CR arrival directions. However, the energy dependent distance cutoff of high energy CRs, shown in Fig. 1, implies that the differential CR flux is dominated at different energies by sources which lie at different distances. Therefore, analyzing the angular distribution of CRs at different energy ranges would provide information on the LSS at different distances, and would therefore probe the 3-dimensional LSS. The exposure which would be required in order to extract 3-dimensional LSS information from the CR arrival distribution may be estimated as follows. Let us assume that we are interested in a LSS feature that lies within a distance range $d_1 - d_2$ and occupies a solid angle $\delta\Omega$. Let's denote the fraction of the flux in the energy range

$E_1 - E_2$, that is contributed on average (i.e. for homogeneous source distribution) by sources within the distance range $d_1 - d_2$, by $f(E_1, E_2, d_1, d_2)$. Our "signal" in the energy range $E_1 - E_2$, i.e. the number of CRs in this energy range that are produce by sources that lie within the LSS feature of interest, is then given by $\sim f(E_1, E_2, d_1, d_2) N(E_1, E_2) \delta\Omega/\mathrm{d}\Omega$, where $N(E_1, E_2)$ is the total number of events in the $E_1 - E_2$ range and $\mathrm{d}\Omega$ is the experimental field of view. The "noise" from sources outside $d_1 - d_2$ is $\sim [(1-f)N\delta\Omega/\mathrm{d}\Omega]^{1/2}$, so that the signal to noise is $\sigma(E_1, E_2, d_1, d_2) \simeq f[N\delta\Omega/\mathrm{d}\Omega(1-f)]^{1/2}$. Figure 7 shows a contour map of the signal to noise $\sigma(E_1, E_2)$ for a structure with radial extent of 50Mpc and angular extent of $10^\circ \times 10^\circ$ lying at a distance of $d = (d_1 + d_2)/2 = 200$, 300Mpc. For this figure, the exposure was chosen to be the current Fly's Eye exposure. The map shows that, as indicated by Fig. 1, the best signal to noise is obtained by choosing the energy range $5.5 - 6.5 \times 10^{19}$eV for $d = 200$Mpc, and $4.5 - 5.5 \times 10^{19}$eV for $d = 300$Mpc. Unfortunately, the exposure required to obtain a signal to noise of order 1 is very large, ~ 300 times the current Fly's Eye exposure, which correspond to $\gtrsim 10$ observation years of the proposed Auger detectors. Thus, although it is possible in principle to probe the 3-dimensional LSS using UCHERs at different energy channels, it is not clear if it would be possible to do so in practice, even with the largest detectors planned today.

We thank Jordi Miralda-Escudé and John Bahcall for valuable suggestions and comments, A. A. Watson for information on the Haverah Park experiment, and P. Sommers for information on the Fly's Eye experiment. EW thanks the Institute for Theoretical Physics (UC Santa-Barbara) for its hospitality. This research was partially supported by a W. M. Keck Foundation grant and NSF grants PHY 95-13835, PHY94-07194.

REFERENCES

*Catalogue of Highest Energy Cosmic Rays, World Data Center for Cosmic Rays, Ins. of Physical and Chemical Research, Itabashi, Tokyo, No. 1

Aharonian, F. A., and Cronin, J. W. 1994, Phys. Rev. D, 50, 1892

Bird, D. J., *et al.* 1994, ApJ, 424, 491

Corbató, S. C., *et al.* 1992, Nucl. Phys. B (Proc. Suppl.) 28B, 36

Cronin, J. W. 1992, Nucl. Phys. B (Proc. Suppl.) 28B, 213

Efstathiou, G. P., Bond, J. R., and White, S. D. M. 1992, MNRAS, 258, 1

Fisher, K. B., *et al.* 1995, ApJS, 100, 67

Greisen, K. 1966, Phys. Rev. Lett., 16, 748

Kronberg, P. P. 1994, Rep. Prog. Phys. 57, 325

Raychaudhury, S., Fabian, A. C., Edge, A. C., Jones, C., & Forman, W. 1991, MNRAS, 248, 101

Shaver, P. A. and Pierre, M. 1989, AA, 220, 35

Stanev, T. *et al.* 1995, Phys. Rev. Lett., 75, 3056

Vallee, J. P. 1990, ApJ, 360, 1

Watson, A. A. 1991, Nucl. Phys. B (Proc. Suppl.) 22B, 116

Watson, A. A. 1993, Inst. Phys. Conf. Ser. 133 (Int. Conf. on Nuclear and Particle Phys., Glasgow), 135

Waxman, E. 1995a, Phys. Rev. Lett. 75, 386

Waxman, E. 1995b, ApJ, 452, L1

Waxman, E. 1995c, to appear in The proceedings for the Third Huntsville Symposium on Gamma-Ray Bursts, eds. C. Kouveliotou, M. Briggs, and J. Fishman (AIP)

Yoshida, S., *et al.* 1995, Astropar. Phys. 3, 151

Zatsepin, G. T., and Kuzmin, V. A. 1966, JETP lett., 4, 78

Table 1. Monte Carlo Results

Model	$> E$ Eev	b^{G}_{RMS}		b^{SG}_{RMS}		$\langle\|b^{G}\|\rangle$		$\langle\|b^{SG}\|\rangle$	
Data	40	46.5	—	23.3	—	39.5	—	18.6	—
I ($\bar{s}_0 = 10^{-2}$)	40	37.3	0.980	33.8	0.007	30.1	0.984	27.3	0.010
I ($\bar{s}_0 = 10^{-4}$)	40	37.2	0.971	33.8	0.009	30.0	0.974	27.4	0.017
UB ($\bar{s}_0 = 10^{-2}$)	40	40.4	0.926	31.5	0.023	33.9	0.907	25.2	0.032
UB ($\bar{s}_0 = 10^{-4}$)	40	40.4	0.895	31.4	0.032	34.0	0.875	25.2	0.050
B ($\bar{s}_0 = 10^{-2}$)	40	38.6	0.961	32.1	0.017	31.3	0.970	25.5	0.027
B ($\bar{s}_0 = 10^{-4}$)	40	38.0	0.947	32.2	0.021	30.9	0.951	25.7	0.035
Data	60	52.7	—	23.9	—	45.9	—	18.2	—
I ($\bar{s}_0 = 10^{-2}$)	60	38.0	0.977	34.5	0.050	30.1	0.987	27.4	0.053
I ($\bar{s}_0 = 10^{-4}$)	60	38.1	0.955	34.5	0.083	30.2	0.972	27.4	0.085
UB ($\bar{s}_0 = 10^{-2}$)	60	42.8	0.922	29.8	0.170	35.7	0.938	23.3	0.169
UB ($\bar{s}_0 = 10^{-4}$)	60	43.0	0.876	29.6	0.227	35.8	0.895	23.1	0.228
B ($\bar{s}_0 = 10^{-2}$)	60	47.5	0.729	16.7	0.957	39.1	0.806	13.2	0.944
B ($\bar{s}_0 = 10^{-4}$)	60	38.5	0.886	17.9	0.863	31.5	0.920	14.1	0.822

Numbers to the right reflect the percentage of 10,000 Monte-Carlo runs which had values as low the data.

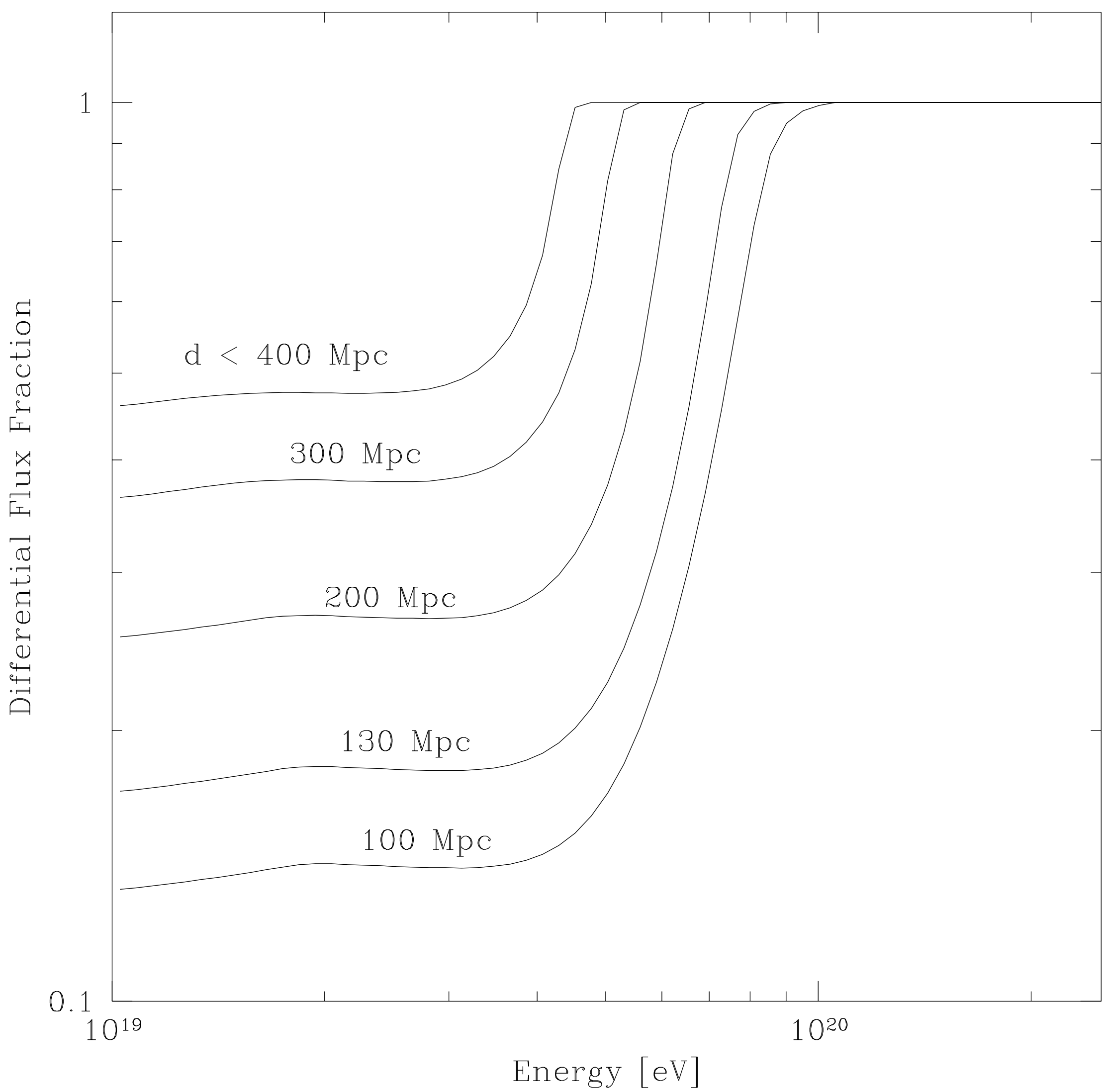

Fig. 1.— The fraction of the differential cosmic ray flux contributed by a homogeneous distribution of sources with distances $< d$ for $d = 100$, 130, 200, 300, and 400 Mpc. The sharp rise in the curves with energy arises from rapid energy loss associated with pion production.

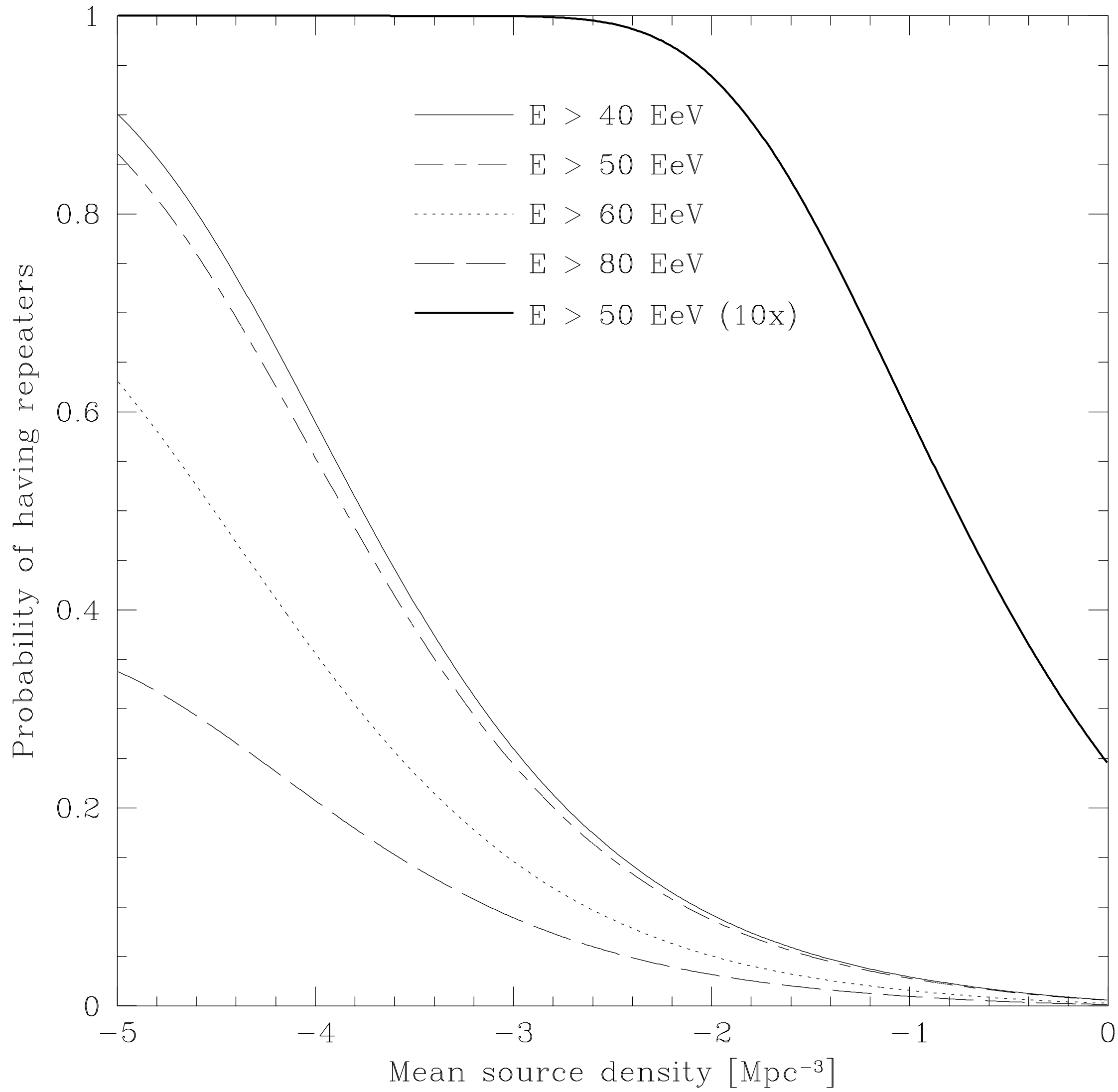

Fig. 2.— The probability of having sources producing more than one CR events (repeaters) as a function of mean CR source density for the Fly's Eye exposure. The light curves denote the probabilities associated with cumulative energy thresholds of 40 (solid), 50 (long-short dashed), 60 (dotted), and 80 (dashed) EeV. The heavy solid curve denotes the probability with a threshold of 50 EeV but with an exposure ten times the current Fly's Eye exposure.

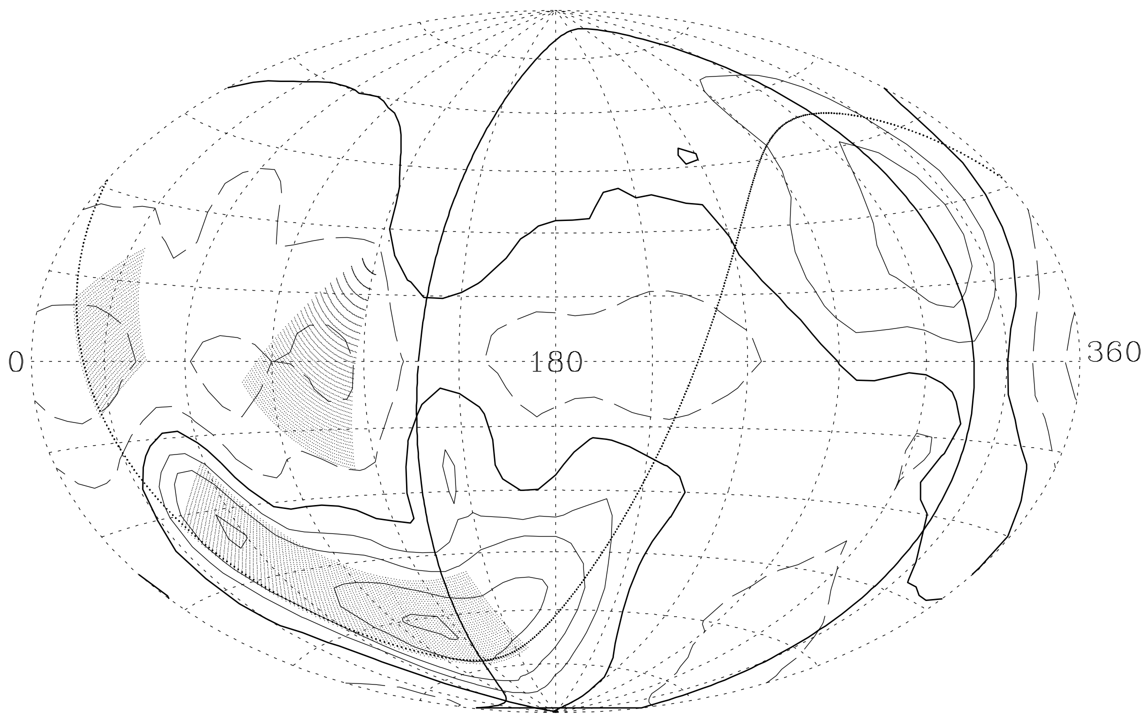

Fig. 3.— Aitoff projection of the fluctuations in the average CR intensity, $\Delta(E, \hat{\Omega})$, for $E = 60$ Eev. The sky coverage was taken to be uniform and the CR sources were assumed to trace the LSS ($b[\delta\rho] = 1 + \delta$). The heavy curve denotes the zero contour. Solid (dashed) contours denote positive (negative) fluctuations at intervals $[-0.5,\ -0.25,\ 0,\ 0.25,\ 0.50,\ 1.0,\ 1.5]$. The Supergalactic plane is denoted by the heavy solid curve roughly perpendicular to the Galactic plane. The dotted curve denotes the Fly's Eye coverage of declination $> -10°$. The shaded regions show the high and low density regions used in the $X(E)$ statistic (equation 5).

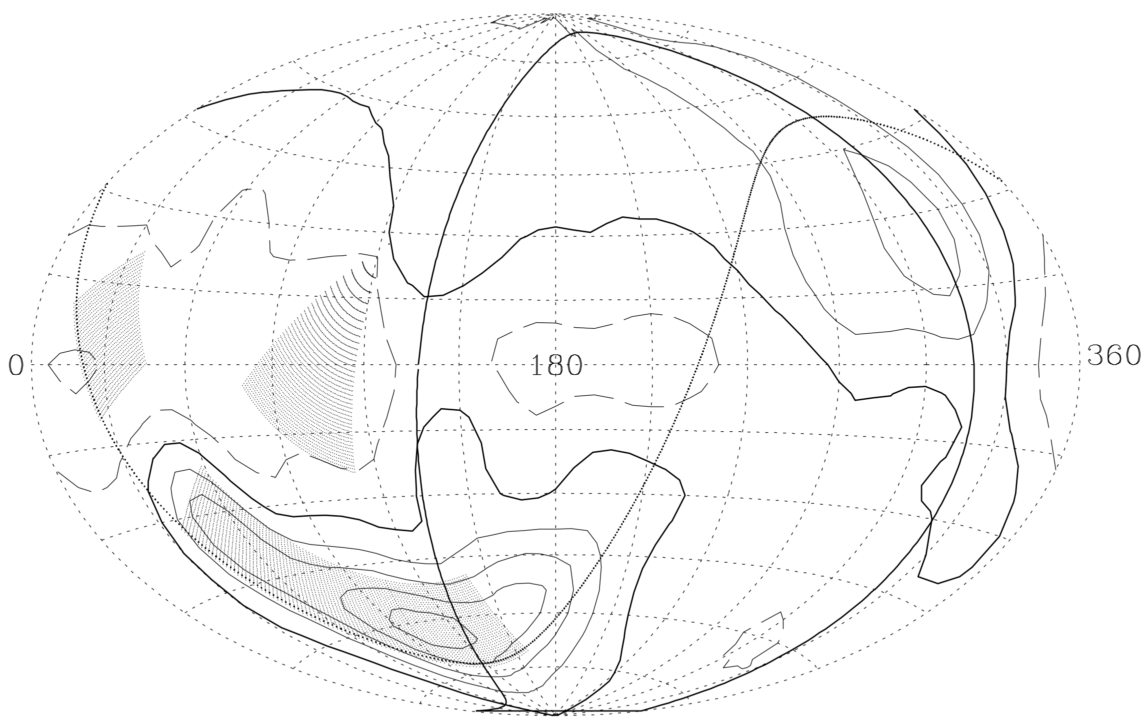

Fig. 4.— Same as Fig. 3, for $E = 40$ EeV. The heavy curve denotes the zero contour. Solid (dashed) contours denote positive (negative) fluctuations at intervals $[-0.4,\ -0.2,\ 0,\ 0.2,\ 0.4,\ 0.6,\ 0.8]$.

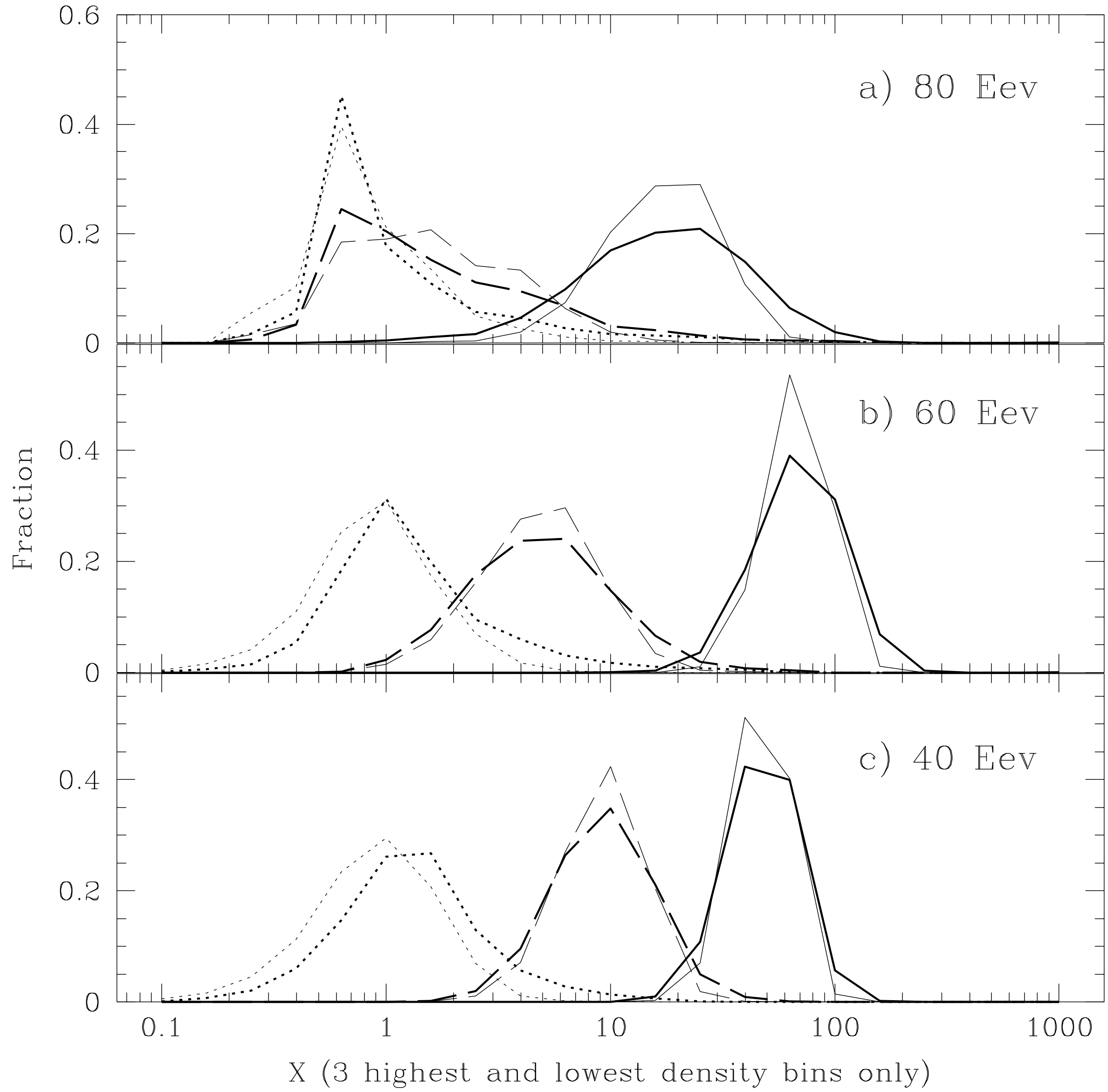

Fig. 5.— Probability distribution of the statistic $X(E)$ (equation 5) for cumulative energies of a) 80, b) 60, and c) 40 Eev computed from 10,000 Monte Carlo realizations of the Fly's Eye detector with 10 times its current exposure. In each panel the solid curves denote the biased model (B), while the dashed curves represent the unbiased model (UB), and the dotted curves are the isotropic (I) model. The light set of curves correspond to a mean CR source density of $\bar{s}_0 = 10^{-2}\mathrm{Mpc}^{-3}$ while the heavier curves correspond to $\bar{s}_0 = 10^{-4}\mathrm{Mpc}^{-3}$.

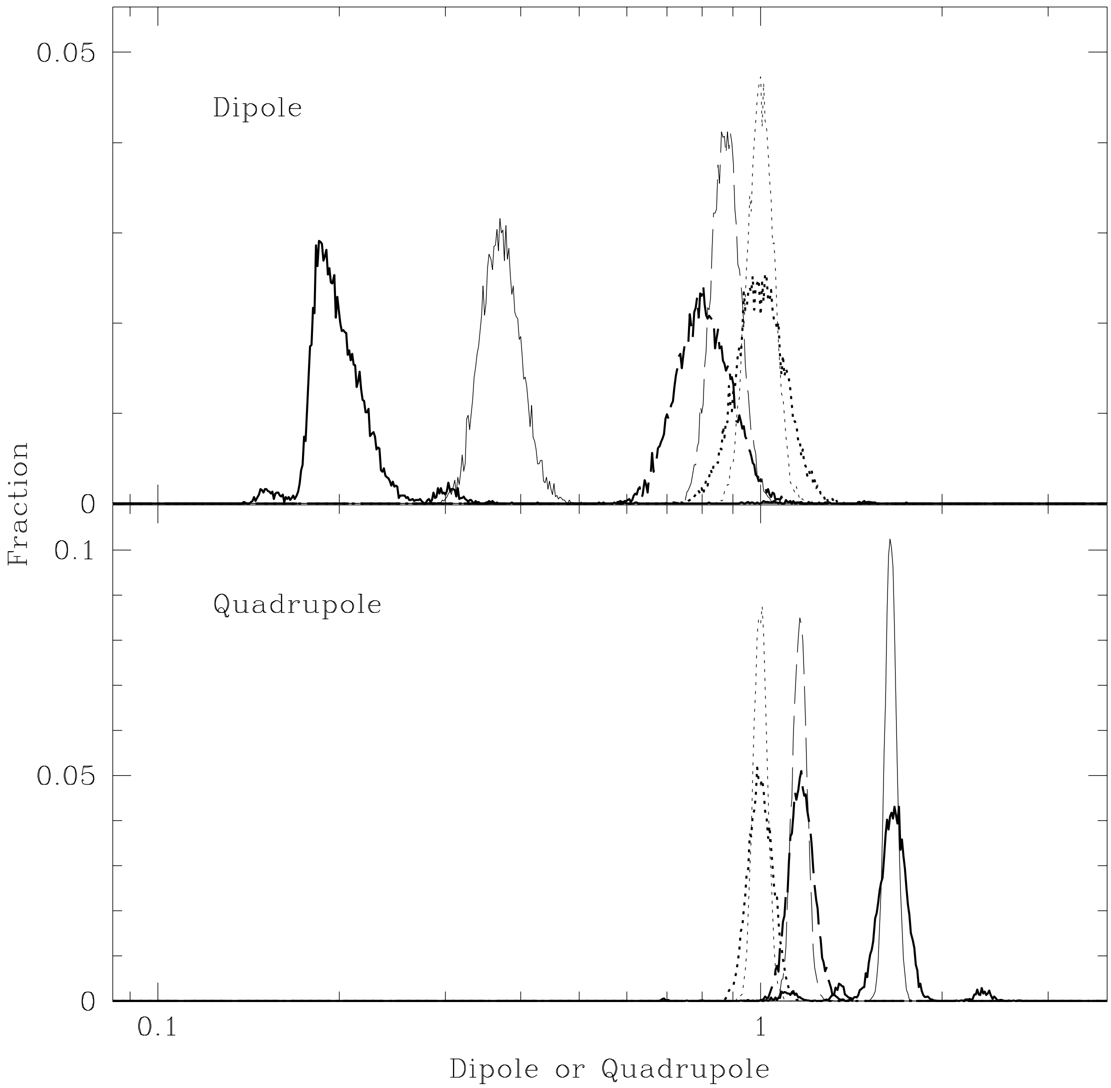

Fig. 6.— Probability distribution of the dipole and quadrupole moments of the CR distribution computed from 10,000 Monte-Carlo realizations of proposed full-sky Auger detector with an effective exposure of 100 times the current Fly's Eye exposure and a cumulative energy threshold of 60 EeV. The various line types correspond to the models the same as in figure 4.

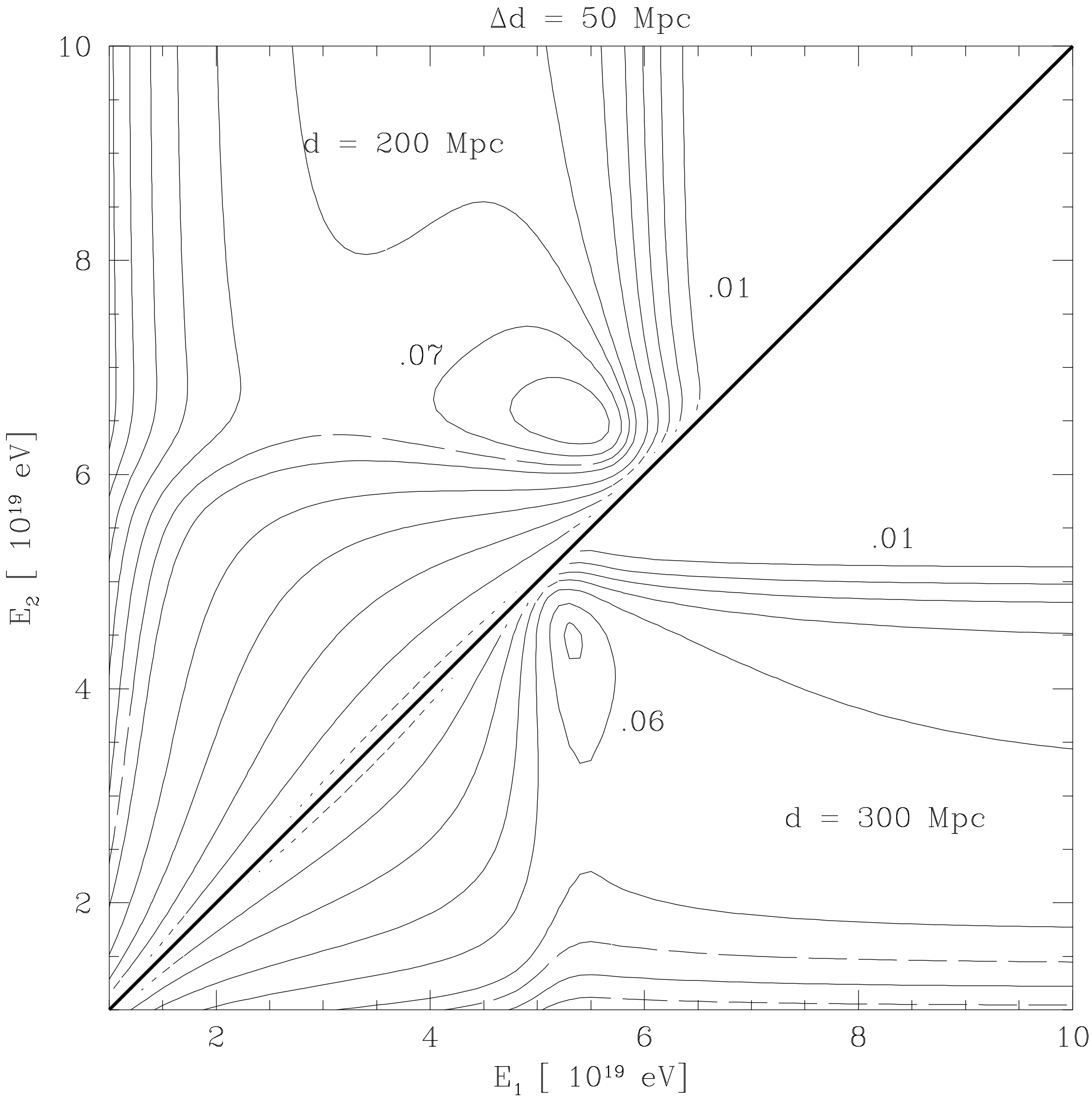

Fig. 7.— Signal to noise contours, $\sigma(E_1, E_2, d_1, d_2)$, for the energy interval corresponding to E_1 and E_2 and a distance resolution of $d_2 - d_1 = 50$ Mpc. The upper panel shows the contours appropriate for probing structures at $(d_1 + d_2)/2 = 200$ Mpc, while the lower panel is "tuned" to $(d_1 + d_2)/2 = 300$ Mpc. The solid contours are spaced at $\Delta\sigma = 0.01$. The dashed contours are at $\sigma = 0.065$ and 0.075.